ISSN 0023-1584, Kinetics and Catalysis, 2007, Vol. 48, No. 1, pp. 93–102. © MAIK "Nauka/Interperiodica" (Russia), 2007.
Original Russian Text © P.V. Snytnikov, V.D. Belyaev, V.A. Sobyanin, 2007, published in Kinetika i Kataliz, 2007, Vol. 48, No. 1, pp. 100–109.

Kinetic Model and Mechanism of the Selective Oxidation of CO in the Presence of Hydrogen on Platinum Catalysts

P. V. Snytnikov, V. D. Belyaev, and V. A. Sobyanin

Boreskov Institute of Catalysis, Siberian Branch, Russian Academy of Sciences, Novosibirsk, 630090 Russia

E-mail: pvsnyt@catalysis.nsk.su

Received April 8, 2005

Abstract—The reaction kinetics of the selective oxidation of carbon monoxide in the presence of hydrogen on a Pt/carbon support catalyst was studied. It was found that this catalyst exhibited high activity and decreased the concentration of CO in a hydrogen-containing gas from 0.6–1.0 vol % to less than 10 ppm at the inlet concentration ratio O_2/CO = 1.0–1.5. A kinetic model of the reaction was proposed to describe quantitatively the experimental results.

DOI: 10.1134/S0023158407010132

INTRODUCTION

In the last few years, the development and commercialization of power systems based on proton-exchange membrane fuel cells (PEMFCs) has been intensively studied around the world [1, 2]. This is due to the well-known and previously demonstrated advantages of fuel cells over commonly used power sources. These are the high efficiency of converting chemical fuel energy into electric energy; noiseless operation; and modular construction, which provides an opportunity to build easily and rapidly PEMFCs with different powers within the framework of the same technology. Hydrogen serves as fuel for PEMFCs, whereas atmospheric oxygen is used as an oxidizing agent. In this case, only water vapor is emitted into the atmosphere during the operation of a fuel cell; this is consistent with the highest environmental standards. In many countries, the improvement of various power supply systems (from cell phones and automobiles to apartment houses) is associated with PEMFCs (although they remain expensive devices).

At the same time, the widespread use of PEMFCs is restricted by a number of difficulties, mainly due to the absence of a developed infrastructure for the hydrogen supply of fuel cells and the unsolved problems of safe hydrogen storage. In this context, the development of a fuel processor—a device for the on-site generation of hydrogen, which is required for the operation of PEMFCs, from hydrocarbon materials (natural gas, gasoline, methanol, ethanol, etc.)—is of paramount importance. The most important studies in this area are currently in progress.

The generation of hydrogen in a fuel processor is performed in several stages. Initially, a hydrocarbon material is converted into a hydrogen-containing mixture, which usually consists of H_2, CO_2, CH_4, N_2, H_2O, and ~0.5–2 vol % CO, using steam, air, or autothermal conversion followed by the water gas shift reaction of carbon monoxide. However, this mixture cannot be used for feeding PEMFCs because carbon monoxide in concentrations higher than 0.001–0.01 vol % (10–100 ppm) is a poison for a fuel electrode [1, 2]. Therefore, to decrease the concentration of CO to 10 ppm, the deep purification of the hydrogen-containing gas is performed at the second stage. The use of the selective catalytic reaction of carbon monoxide oxidation in the presence of H_2 is most promising among the currently available purification techniques. In the course of this purification, the following two catalytic reactions (CO oxidation and H_2 oxidation) occur simultaneously:

$$2CO + O_2 \longrightarrow 2CO_2,$$

$$2H_2 + O_2 \longrightarrow 2H_2O(\text{gas}).$$

The intensity of these reactions is commonly characterized by the degrees of conversion of CO (X_{CO}) and O_2 (X_{O_2}) and the selectivity (S), the ratio between the amounts of oxygen consumed for the oxidation of CO and oxygen consumed in both of the reactions.

One of the most active and selective catalysts proposed for this reaction is platinum supported onto aluminum oxide [3–8], zeolites [8–11], or a Sibunit graphite-like carbon material [12–15]. The majority of these catalysts operate at 150–200°C.

Although the reaction of catalytic CO oxidation in the presence of hydrogen has been studied for a long time, the ideas of its mechanism are incomplete and often descriptive. The mechanism of this reaction was discussed in a few publications [16–18]. Kahlich et al. [16] studied the kinetics of CO oxidation in the presence of H_2 on a 0.5 wt % $Pt/\gamma\text{-}Al_2O_3$ catalyst. The experiments were performed at 150–250°C with the use of model gas mixtures containing 0.02–1.5 vol % CO, 0.01–2.25 vol % O_2, 75 vol % H_2, and N_2

Table 1. Physicochemical characteristics of catalysts

Catalyst	S_{sp}, m^2/(g Cat)	V_{pore}, cm^3/(g Cat)	Active component precursor	D_M	S_M, m^2/(g Cat)	d_M, nm
1 wt % Pt/C	300	0.3	$H_2[Pt_3(CO)_6]_5$	0.8	2	1.4
2 wt % Pt/γ-Al_2O_3	150	0.5	$Pt(NO_3)_4$	0.55	2.8	2.0

(to Σ100%). The apparent activation energy of the reaction E = 71 kJ/mol and the orders of reaction with respect to carbon monoxide (q_{CO} = –0.4) and oxygen (q_{O_2} = +0.8) were determined. Kim and Lim [17] obtained the following similar values for this reaction occurring on Pt/γ-Al_2O_3: E = 78 kJ/mol, q_{CO} = –0.51, and q_{O_2} = +0.76. Kahlich et al. [16] reasonably noted that, on this catalyst, the apparent kinetic characteristics (E, q_{CO}, and q_{O_2}) of CO oxidation were identical both in the presence of H_2 and without hydrogen when the surface of Pt was almost completely covered with CO. On this basis, the conclusion was drawn that the surface of platinum was also almost completely covered with adsorbed CO molecules in the course of the reaction of CO oxidation in the presence of H_2 and the mechanism of this reaction is not different in principle from the Langmuir–Hinshelwood mechanism, which occurs in the reaction of CO oxidation without H_2. In this context, note that Schubert et al. [18], who used Fourier transform IR spectroscopy, demonstrated that, indeed, the surface of platinum was completely covered with CO in the oxidation of CO in the presence of H_2 on Pt/γ-Al_2O_3.

In this work, we studied the reaction kinetics of CO oxidation in hydrogen-containing mixtures on platinum catalysts supported on a Sibunit carbon material [19] and aluminum oxide (Pt/C and Pt/Al_2O_3, respectively), proposed a reaction mechanism, and found specific features in the oxidation of CO in the presence of H_2. In accordance with the mechanism proposed, a mathematical model for the occurrence of the reaction in a plug-flow reactor was formulated and analyzed. A reactor of this type most closely corresponds to the reactor used in this study for kinetic experiments. The results of analysis are used to describe experimental kinetic data on the reaction of CO oxidation in the presence of H_2, which were obtained on Pt/C and Pt/γ-Al_2O_3 catalysts in this work.

EXPERIMENTAL

Preparation of Catalysts

A Sibunit graphite-like carbon material (spherical granules ~1 mm in diameter; specific surface area S_{sp} = 300 m^2/g; pore volume of 0.3 cm^3/g) and γ-Al_2O_3 (spherical granules ~1 mm in diameter; specific surface area S_{sp} = 150 m^2/g; pore volume of 0.5 cm^3/g) were used as supports for the Pt/C and Pt/γ-Al_2O_3 catalysts, respectively.

The Pt/C catalyst was prepared in accordance with a published procedure [20]. A required amount of the support was placed in a flask with acetone, and the contents were evacuated to remove air from the pores of the support. Then, the flask was filled with carbon monoxide, and a calculated amount of an acetone solution of the platinum carbonyl cluster $H_2[Pt_3(CO)_6]_5$ with a concentration of 5.7 mg Pt/ml was added with intense stirring. After stirring the suspension for 2 h, the solution was poured out and the catalyst was dried in air at 80°C for 2 h and then reduced with hydrogen at 300°C for 2 h. The platinum content of the sample was 1 wt %.

The Pt/γ-Al_2O_3 catalyst was prepared by the incipient wetness impregnation of γ-Al_2O_3 with an aqueous solution containing platinum nitrate ($Pt(NO_3)_4$) and nitric acid. The solution was added to the support in several portions and evaporated to an air-dry state with stirring. The resulting sample was dried in air for 1 h at 120°C; next, the sample was kept in a flow of nitrogen at 200°C for 4 h and reduced in a flow of hydrogen at 300°C for 2 h. The platinum content of the sample was 2 wt %.

Physicochemical Characteristics of the Catalysts

The catalysts prepared were characterized by a set of physicochemical techniques (Table 1).

The Pt content of supported catalysts was determined by gravimetry. The specific surface areas (S_{sp}) and pore volumes (V_{pore}) of supports and catalysts were determined from the total isotherms of low-temperature nitrogen adsorption at 77 K, which were measured on an ASAP-2400 instrument (Micrometrics, United States).

The dispersity, surface area, and average particle size of metals in the supported Pt catalysts were determined using the adsorption of CO in accordance with a published procedure [21]. The dispersity of metals was calculated based on the assumption that one CO molecule is adsorbed at one Pt atom. Table 1 summarizes the physicochemical characteristics of the test catalysts: total specific surface area (S_{sp}), pore volume (V_{pore}), dispersity (D_M), specific surface area of the supported metal (S_M), and particle size (d_M). They were equal to one another for catalyst samples characterized before and after experiments; this suggested the stability of catalysts under reaction conditions. The values of S_{sp} and V_{pore} for all of the catalysts were equal to the values of S_{sp} and V_{pore} for the supports.

The catalysts were studied by transmission electron microscopy on a JEM-2010 electron microscope from

JEOL (Japan) at an accelerating voltage of 200 kV. Figure 1 shows a typical micrograph of the Pt/C catalyst. It can be seen that small platinum particles of size ~1–4 nm were present in the catalyst; this is consistent with the average particle size of Pt (1.4 nm) calculated from the dispersity (see Table 1).

The composition and surface state of catalysts were studied by XPS. The XPS spectra were measured on a VG ESCALAB electron spectrometer from VG Scientific (United Kingdom) (AlK_α radiation; average free path of electrons, 20–30 Å, depending on the test line) under conditions of a retarding potential with a constant energy of electron transmission through a hemispherical analyzer. The XPS spectra were calibrated using the C 1*s* line (E_b = 284.4 eV). The concentration ratio between catalyst components was determined from corresponding line intensities in the spectrum with consideration for tabulated atomic sensitivity factors of the elements [22, 23]. The XPS spectra obtained before and after kinetic experiments were identical. The analysis of the electronic state of platinum in the 1 wt % Pt/C catalyst was performed using the Pt 4*f* line. The spectrum exhibited a doublet with $E_b(Pt4f_{7/2})$ = 71.4 eV. According to reference data [22, 23], this value corresponds to platinum metal. For the 2 wt % Pt/γ-Al_2O_3 catalyst, the analysis of the state of platinum was performed using the Pt 4*d* line because the Pt 4*f* line interferes with the intense Al 2*p* line from the support. The Pt 4*d* line is characterized by $E_b(Pt\ 4d_{5/2})$ = 314.2 eV. According to reference data [22, 23], this value of E_b corresponds to platinum in a metal state.

Kinetic Experiments and Data Processing

The reaction of CO oxidation in hydrogen-containing gases was studied in a quartz flow reactor at atmospheric pressure. The reactor was a *U*-shaped tube 40 cm in length with an inner diameter of 8 mm and a wall thickness of ~1 mm. A thermocouple well with an outer diameter of 3 mm was arranged at the center along the reactor axis. A catalyst (pellet diameter of ≤1 mm), which was premixed with quartz powder (particle size of ~1 mm), was placed in the reactor. The catalyst bed thickness was 12 cm. A filter was placed at the reactor inlet and outlet in order to exclude the entry of small catalyst particles with a gas flow into the capillary system of gas inlet and outlet lines. The temperature was measured with a Chromel–Alumel thermocouple placed in the well at the center of the catalyst bed. In the course of experiments, temperature changes across the catalyst bed were usually no greater than 2 K. The catalysts were not pretreated before the experiments.

The concentrations of reactants and reaction products at the reactor inlet and outlet were analyzed with the use of two Tsvet 530 chromatographs equipped with a column with NaX molecular sieves and a column with Porapak Q. The sensitivity of analysis allowed us to measure the concentrations of CO, CH_4, and CO_2 to a level of ~10^{-4} vol % or O_2 to ~10^{-3} vol %. The conversions of CO and O_2 and selectivity were calculated from the equations

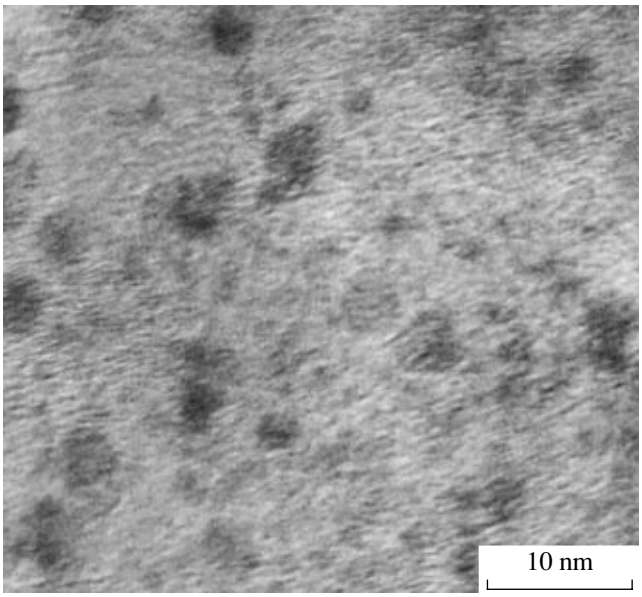

Fig. 1. Electron micrograph of the 1 wt % Pt/C catalyst. Dark spots: metal particles.

$$X_{CO} = \frac{[CO]_0 - [CO]}{[CO]_0} \times 100\%;$$

$$X_{O_2} = \frac{[O_2]_0 - [O_2]}{[O_2]_0} \times 100\%;$$

$$S = \frac{1}{2}\frac{[CO]_0 - [CO]}{[O_2]_0 - [O_2]} \times 100\%;$$

where $[CO]_0$ and $[O_2]_0$ are the concentrations of CO and O_2, respectively, at the reactor inlet and [CO], $[CO_2]$, and $[O_2]$ are the concentrations of CO, CO_2, and O_2, respectively, at the reactor outlet.

To avoid errors in the determination of concentrations in the course of kinetic experiments, we checked the balance on carbon

$$[CO]_0 = [CO] + [CO_2].$$

In all of the experiments, the deviation from a balance on carbon was no higher than ±5 rel %.

Kinetic Experiments with the Use of In Situ IR Spectroscopy

Kinetic experiments with the use of in situ Fourier transform IR spectroscopy were performed for a detailed study of the mechanism of catalytic oxidation of CO in hydrogen-containing gas mixtures. For this purpose, a heated flow cell (reactor) with an optical path length of 1 mm was made in order to decrease the contribution of gas-phase CO molecules to the total spectrum. Windows of CaF_2 glued with a high-temper-

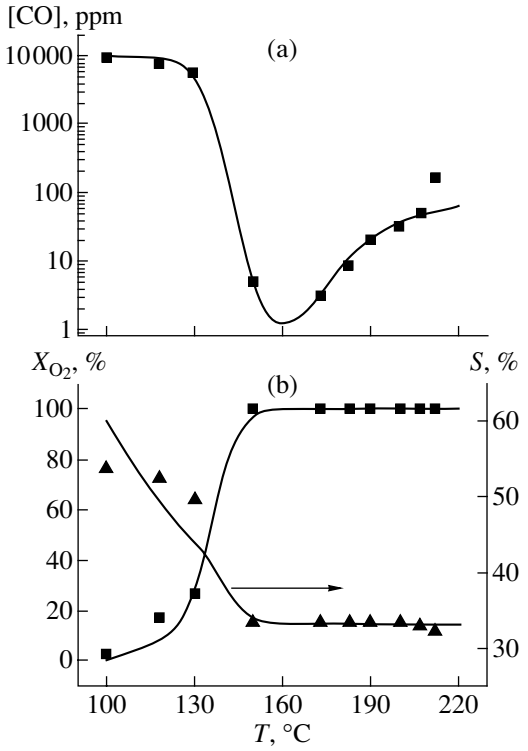

Fig. 2. Dependence of (a) the outlet concentration of CO or (b) the conversion of O_2 and selectivity on the reaction temperature of CO oxidation in the presence of H_2 on the 1 wt % Pt/C catalyst. The composition of the mixture at the reactor inlet, vol %: CO, 1; O_2, 1.5; H_2, 75; He, 22.5. Space velocity: 12000 h^{-1}. Points and lines refer to experimental and calculated data, respectively.

ature hermetic were used in the cell. A catalyst as a pressed pellet (1 × 2 cm) ~0.1 mm in thickness was placed in the cell. The reaction gas mixture was supplied and removed through capillaries inserted into the cell. A heating coil and a Chromel–Alumel thermocouple for temperature measurements were attached to the outside of the cell. The cell was placed in a Shimadzu FTIR-8300 spectrometer. The spectra were recorded with a resolution of 4 cm^{-1} at 50 scans per spectrum. The time taken to record a spectrum was ~1 min. The concentrations of reactants and reaction products at the reactor inlet and outlet were determined by chromatography. The state of adsorbed CO molecules on catalyst surfaces was monitored by measuring absorption bands in the region 1800–2300 cm^{-1}, which corresponds to the vibrations of CO in its complexes with metals [24]. The surface coverage with adsorbed CO molecules (θ_{CO}) was determined from absorption band intensities: $\theta_{CO} = I/I_0$, where I and I_0 are the absorption band intensities corresponding to adsorbed CO molecules in the course of a kinetic experiment and in a monolayer coverage of the catalyst surface, respectively.

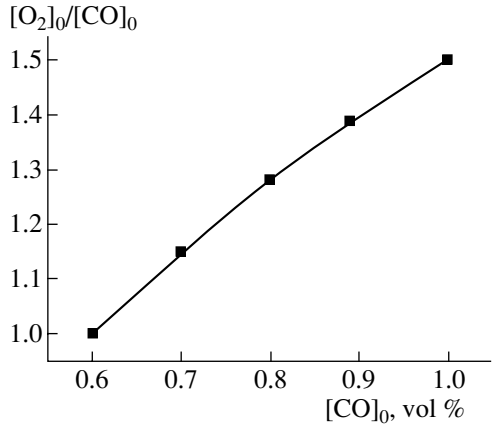

Fig. 3. Dependence of the O_2/CO ratio on the initial concentration of CO in a hydrogen-containing gas in the course of oxidation on the 1 wt % Pt/C catalyst. Space velocity: 7500 h^{-1}.

RESULTS AND DISCUSSION

Oxidation of CO on Pt/C in the Presence of H_2

The experiments were performed with a gas mixture containing 1 vol % CO, 1.5 vol % O_2, and 97.5 vol % H_2. The formation of methane in the course of the experiment was not observed.

According to the results shown in Fig. 2, the outlet concentration of CO decreased with temperature and reached values lower than 10 ppm in the range 150–185°C. A further increase in the temperature resulted in a gradual increase in the concentration of CO at the reactor outlet. The conversion of O_2 increased with temperature and reached 100% at 150°C; thereafter, it remained constant. As the temperature was increased, the selectivity monotonically decreased from 75 to 33%. Thus, there is a temperature range over which the required level of purification is not achieved.

Note that the amount of oxygen at the reactor inlet was three times higher than that stoichiometrically required for the oxidation of CO. However, this value $[O_2]_0$ is a minimum value required for decreasing the CO concentration from 1 vol % to 10 ppm. Therefore, the O_2/CO inlet concentration ratio necessary for decreasing the carbon monoxide concentration to the required level is a key parameter of the selective CO oxidation reaction. Figure 3 shows the dependence of this parameter on the inlet concentration of CO. In the experiments with gas mixtures containing 0.6–1.0 vol % CO, 0.6–1.5 vol % O_2, and 97.5–98.8 vol % H_2 at 140–160°C, the conversion of oxygen was equal to 100%.

The O_2/CO ratio increased almost linearly with the inlet concentration of CO, and it was higher than the minimum value (equal to 0.5) stoichiometrically required for the reaction of CO oxidation to CO_2 by a factor of 2–3.

Table 2. Published reaction rate constants of the separate oxidation of H_2 and CO [25–30]*

k_i	k_0, s^{-1} atm^{-1}	$k_0 \times 10^{-13}$, s^{-1}	E_0, kcal/mol	E, kcal/mol	x
k_1	1.6×10^8	–	–	–	–
k_2	1.5×10^8	–	–	–	–
k_3	6.9×10^5	–	–	–	–
k_{-1}	–	1	34.9	19.9	2
k_{-2}	–	1	19	7	1
k_4	–	100	24.1	12	1
k_5	–	1	5	0	–
k_6	–	1	0	0	–

* The rate constants of the steps of CO, H_2, and O_2 adsorption (k_1, k_2, and k_3, respectively) are independent of temperature. The rate constants of the steps of CO and H_2 desorption (k_{-1} and k_{-2}, respectively) and surface reactions (k_4–k_6) are represented in an Arrhenius form with consideration for the dependence of the activation energy on the surface coverage with reactants (θ): $k_i = k_{i0}\exp[-(E_0 - E\theta^x)/RT]$, where x is an empirical parameter.

Thus, platinum supported on Sibunit is a sufficiently active catalyst for the reaction of CO oxidation in the presence of hydrogen; it decreases the concentration of CO in hydrogen-containing mixtures to the required level of 10 ppm.

Reaction Mechanism and Kinetic Model

It is well known that the oxidation of hydrogen and carbon monoxide on various metal catalysts, including platinum, belongs to the catalytic reactions studied in most detail. Their mechanisms are considered well substantiated [25–30]; at temperatures of ≤400°C, they consist of the following steps:

H_2 oxidation	CO oxidation
$H_{2(g)} \overset{k_2}{\underset{k_{-2}}{\rightleftarrows}} 2H_{(a)}$	$CO_{(g)} \overset{k_1}{\underset{k_{-1}}{\rightleftarrows}} CO_{(a)}$
$O_{2(g)} \xrightarrow{k_3} 2O_{(a)}$	$O_{2(g)} \xrightarrow{k_3} 2O_{(a)}$
$H_{(a)} + O_{(a)} \xrightarrow{k_5} OH_{(a)}$	$CO_{(a)} + O_{(a)} \xrightarrow{k_4} CO_{2(g)}$
$H_{(a)} + OH_{(a)} \xrightarrow{k_6} H_2O_{(g)}$	

The subscripts (g) and (a) refer to the gas phase and the adsorbed state of substances, respectively.

Previously [25–30], the constants of all of the steps were determined (Table 2). It was demonstrated that kinetic data obtained over a wide range of the steady-state and non-steady-state reaction conditions of the separate oxidation of H_2 and CO on Pt-containing catalysts can be satisfactorily interpreted in terms of these mechanisms. In this context, it seemed reasonable to describe the kinetic data on the oxidation of CO in the presence of H_2 on Pt-containing catalysts in terms of the above concepts of the reaction mechanisms of the separate oxidation of H_2 and CO.

Combining the steps of the separate oxidation of H_2 and CO, we can represent the reaction mechanism of CO oxidation in the presence of hydrogen in the following form:

$$CO_{(g)} \overset{k_1}{\underset{k_{-1}}{\rightleftarrows}} CO_{(a)}, \quad \text{(I)}$$

$$H_{2(g)} \overset{k_2}{\underset{k_{-2}}{\rightleftarrows}} 2H_{(a)}, \quad \text{(II)}$$

$$O_{2(g)} \xrightarrow{k_3} 2O_{(a)}, \quad \text{(III)}$$

$$CO_{(a)} + O_{(a)} \xrightarrow{k_4} CO_{2(g)}, \quad \text{(IV)}$$

$$H_{(a)} + O_{(a)} \xrightarrow{k_5} OH_{(a)}, \quad \text{(V)}$$

$$H_{(a)} + OH_{(a)} \xrightarrow{k_6} H_2O_{(g)}. \quad \text{(VI)}$$

Steps (I), (III), and (IV) belong to the reaction of CO oxidation; steps (II), (III), (V), and (VI) belong to the reaction of H_2 oxidation.

Note that the steps of CO_2 and H_2O formation in the proposed mechanism are irreversible. This fact did not allow us to take into account possible effects of water and carbon dioxide on the course of the reaction.

A mathematical model for this reaction mechanism under steady-state conditions in a plug-flow reactor corresponds to the following set of equations:

$$\frac{dn_{CO}}{d\xi} = -g\frac{L_0}{u}(k_1 P n_{CO}(1-\theta) - k_{-1}\theta_{CO}); \quad (1)$$

$$\frac{dn_{H_2}}{d\xi} = -g\frac{L_0}{u}(k_2 P n_{H_2}(1-\theta)^2 - k_{-2}\theta_H^2); \quad (2)$$

$$\frac{dn_{O_2}}{d\xi} = -g\frac{L_0}{u}k_3 P n_{O_2}(1-\theta)^2; \quad (3)$$

$$\frac{dn_{CO_2}}{d\xi} = g\frac{L_0}{u}k_4\theta_{CO}\theta_O; \quad (4)$$

$$\frac{dn_{H_2O}}{d\xi} = g\frac{L_0}{u}k_6\theta_{OH}\theta_H; \quad (5)$$

Table 3. Reaction rate constants of the steps of CO oxidation in the presence of H_2*

k_i	k_0, s^{-1} atm^{-1}	$k_0 \times 10^{-13}$, s^{-1}	E_0, kcal/mol	E, kcal/mol	x
k_1	1.6×10^8	–	–	–	–
k_2	1.5×10^8	–	–	–	–
k_3	9.2×10^4	–	–	–	–
k_{-1}	–	0.8	34.9	18	2
k_{-2}	–	1	19	9	1
k_4	–	70	24.1	9	1
k_5	–	2	10	0	–
k_6	–	1	0	0	–

* The rate constants of the steps of CO, H_2, and O_2 reactant adsorption (k_1, k_2, and k_3, respectively) are independent of temperature. The rate constants of the steps of CO and H_2 desorption (k_{-1} and k_{-2}, respectively) and surface reactions (k_4–k_6) are represented in an Arrhenius form with consideration for the dependence of the activation energy on the surface coverage with reactants (θ): $k_i = k_{i0}\exp[-(E_0 - E\theta^x)/RT]$, where x is an empirical parameter.

$$g = S_{sp} m N_0 \frac{k_B T}{V_{react} P}; \quad (6)$$

$$\frac{d\theta_{CO}}{dt} = 0 = k_1 P n_{CO}(1-\theta) - k_{-1}\theta_{CO} - k_4\theta_{CO}\theta_O; \quad (7)$$

$$\frac{d\theta_H}{dt} = 0 = 2k_2 P n_{H_2}(1-\theta)^2 - 2k_{-2}\theta_H^2 - k_5\theta_H\theta_O - k_6\theta_H\theta_{OH}; \quad (8)$$

$$\frac{d\theta_O}{dt} = 0 = 2k_3 P n_{O_2}(1-\theta)^2 - k_4\theta_{CO}\theta_O - k_5\theta_H\theta_O; \quad (9)$$

$$\frac{d\theta_{OH}}{dt} = 0 = k_5\theta_H\theta_O - k_6\theta_H\theta_{OH}; \quad (10)$$

$$\theta = \theta_{CO} + \theta_O + \theta_H + \theta_{OH}; \quad (11)$$

where θ_i is the surface coverage with the ith substance; k_i are the rate constants of steps; T is the catalyst bed temperature; u is the linear velocity of a gas flow; S_{sp} is the surface area of an active component per unit weight of the catalyst; $N_0 = 1.5 \times 10^{19}$ m^{-2} is the monolayer capacity; P is the reaction pressure; V_{react} is the volume of the catalyst bed; k_B is the Boltzmann constant; L_0 is the length of the catalyst bed; L is the distance from the start of the catalyst bed; n_i is the mole fraction of CO, H_2, O_2, CO_2, or H_2O in a gas; m is the weight of a catalyst sample; and $\xi = L/L_0$.

Equations (1)–(5) reflect the dependence of the concentrations of initial substances and reaction products along the catalyst bed; Eqs. (7)–(10) reflect steady-state conditions for adsorbed intermediate species. Evidently, the dependence of n_i and θ_i on the length of the catalyst bed can be found by solving the set of Eqs. (1)–(11). Then, X_{CO}, X_{O_2}, and the selectivity S can be calculated from the known values of n_i at the reactor inlet and calculated values of n_i at the reactor outlet and compared with experimental values.

Initially, the set of Eqs. (1)–(11) was solved by a numerical method using the rate constants of steps given in Table 2. The dependence of X_{CO}, X_{O_2}, and S upon reaction temperature on the 1 wt % Pt/C catalysts was calculated; it was found that these relationships qualitatively describe the experimental results. For quantitatively describing the experimental results, we varied the parameters (activation energies and preexponential factors) of the rate constants of steps. Table 3 summarizes the final values of the rate constants of steps, which were used in all of the subsequent calculations.

From a comparison between data given in Tables 2 and 3, it follows that they differ from each other only slightly. The calculated and experimental kinetic data and the occurrence of the reaction of CO oxidation in the presence of H_2 on Pt-containing catalysts (1 wt % Pt/C and 2 wt % Pt/γ-Al_2O_3) are considered and discussed below with the use of particular examples.

Interpretation of Kinetic Data Obtained on the 1 wt % Pt/C Catalyst

According to Fig. 2, the theoretical relationships are quantitatively consistent with the experimental data; in particular, the temperature range in which the concentration of CO in a hydrogen-containing gas can be decreased to 10 ppm is the same. This suggests that the model proposed adequately interprets the real course of the reaction.

To examine the occurrence of CO oxidation in the presence of H_2 on the 1 wt % Pt/C catalyst, let us consider the calculated dependence of the surface coverage with adsorbed species ($CO_{(a)}$, $H_{(a)}$, $OH_{(a)}$, and $O_{(a)}$) and the outlet concentrations of CO and O_2 on the length of the catalyst bed. As an example, Fig. 4 shows these

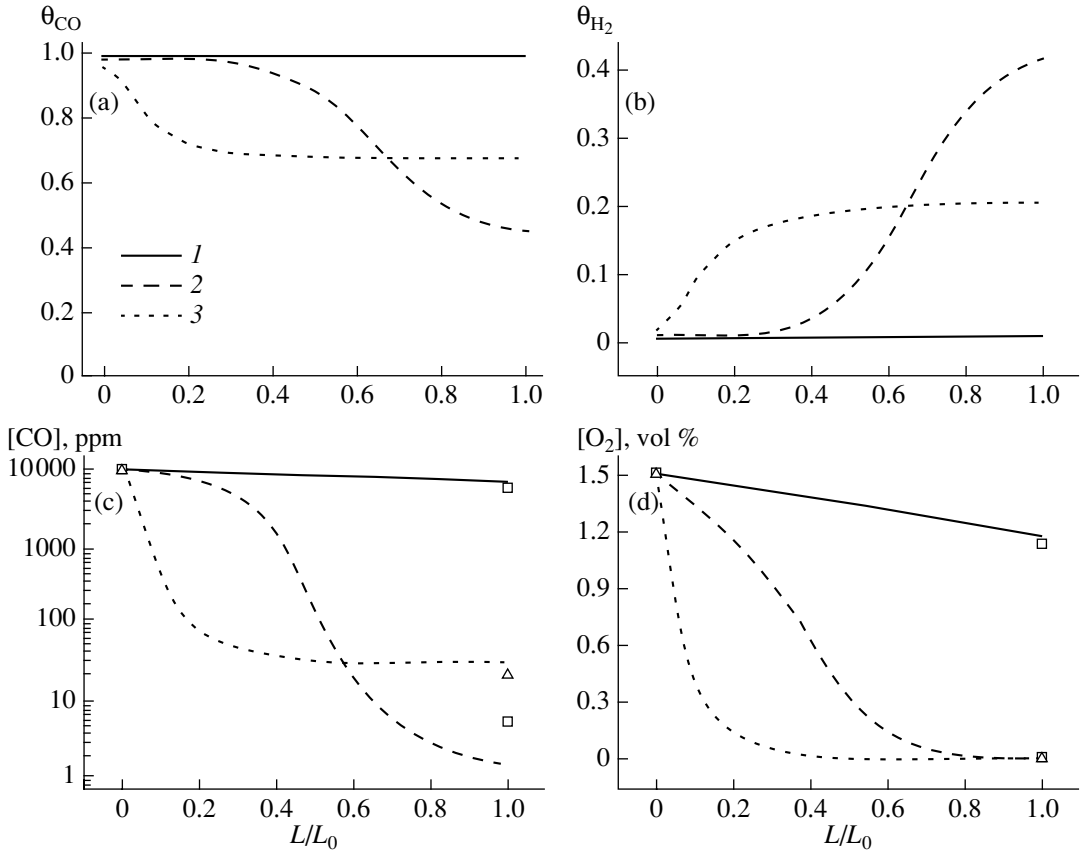

Fig. 4. Dependence of (a) θ_{CO}, (b) θ_{H_2}, and (c, d) reactant concentrations on the value of L/L_0 in the course of the reaction of CO oxidation in the presence of H_2 on the 1 wt % Pt/C catalyst. T = (*1*) 130, (*2*) 150, or (*3*) 190°C. Experimental conditions are specified in Fig. 2. Points and lines refer to experimental and calculated data, respectively.

relationships at the following three characteristic temperatures:

130°C, the temperature at which the conversions of CO and O_2 did not exceed 30%;

160°C, the temperature at which the outlet concentration of CO reached a minimum and the conversion of O_2 was equal to 100%;

190°C, the temperature at which the conversion of O_2 remained equal to 100% and the concentration of CO increased.

Note that the calculated surface coverages with $OH_{(a)}$ and $O_{(a)}$ species were extremely low ($<10^{-7}$ of a monolayer) in all cases, and they are not shown in Fig. 4.

As can be seen in Fig. 4, at 130°C, the catalyst surface was almost completely covered with CO molecules at all of the values of L/L_0, whereas θ_{H_2} was small. In this case, the concentrations of CO and O_2 in the gas phase insignificantly smoothly decreased along the catalyst bed (Figs. 4c, 4d). The reaction was limited by the adsorption of O_2 on the surface of Pt, which was almost completely covered with CO molecules. An increase in the temperature to 150°C had only a slight effect on θ_{CO} and θ_{H_2} to $L/L_0 \le 0.4$; only in the range $L/L_0 \sim 0.4$–0.8 did it result in a decrease of θ_{CO} from ~1 to 0.4 and in an increase of θ_{H_2} from ~0.02 to 0.4 (Figs. 4a, 4b). As a result of this, the concentrations of CO and O_2 in the gas rapidly decreased (to several ppm and ~0, respectively). This dramatic increase in the reaction rates of CO and H_2 oxidation can be explained by an increase in the fraction of the free surface required for the adsorption of O_2. It is interesting to note that, at this temperature, the surface coverage of the operating catalyst with CO molecules was also insignificant; for example, it was 0.4 of a monolayer even at a CO concentration of several ppm. A further increase in the temperature to 190°C resulted in a considerable decrease in θ_{CO} from ~0.95 to 0.7 and an increase in θ_{H_2} from ~0.02 to 0.15 even at the start of the catalyst bed at $L/L_0 < 0.2$. Under these conditions, the rates of H_2 and CO oxidation increased and the selectivity of the reaction decreased; that is, the amount of oxygen that reacted with hydrogen increased, as compared with the fraction of oxygen that reacted with carbon monoxide. Therefore, the concentrations of O_2

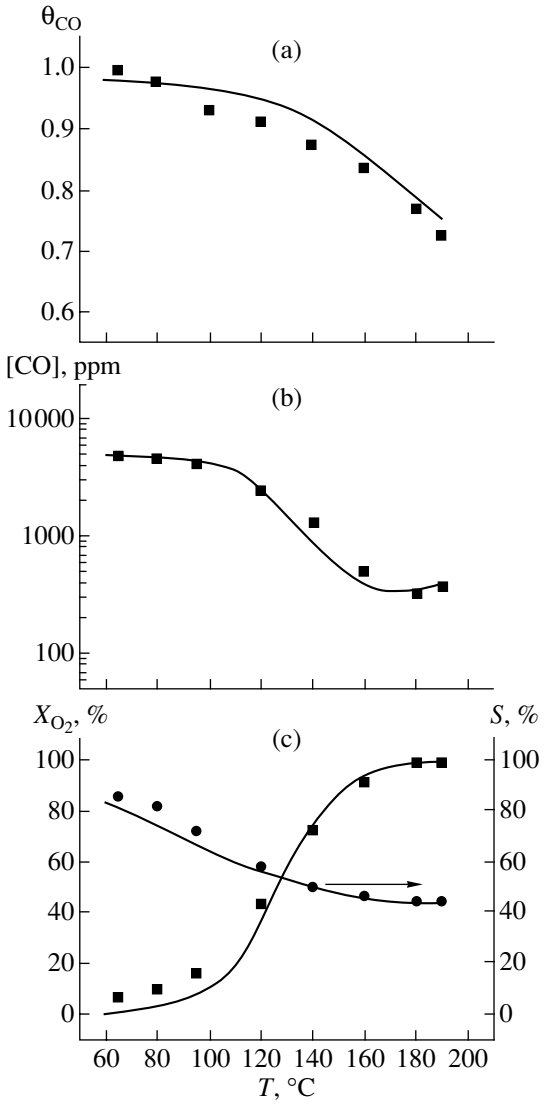

Fig. 5. Dependence of (a) θ_{CO}, (b) the outlet concentration of CO, and (c) the conversion of O_2 or selectivity on temperature in the oxidation of CO in the presence of H_2 on the 2 vol % Pt/Al_2O_3 catalyst. The composition of the mixture at the reactor inlet, vol %: CO, 0.50; O_2, 0.55; H_2, 75; He, 23.95. Space velocity: 12000 h^{-1}. Points and lines refer to experimental and calculated data, respectively.

and CO dramatically decreased (to ~0 and 40 ppm, respectively). Finally, at $L/L_0 > 0.2$, oxygen was completely consumed when the reaction mixture moved along the catalyst bed, whereas the concentration of CO and the values of θ_{CO} and θ_{H_2} remained unchanged. In the course of the reaction, the value of θ_{CO} was ~0.7 of a monolayer. Thus, in the oxidation of CO in the presence of H_2, the surface coverage of the Pt-containing catalyst with CO molecules was significant. This circumstance is of importance for the predominant oxidation of CO in mixtures containing hydrogen with a concentration higher than that of CO by 2–6 orders of magnitude. This conclusion is consistent with published concepts of the course of the reaction and supported by the results considered below, which were obtained using in situ IR spectroscopy.

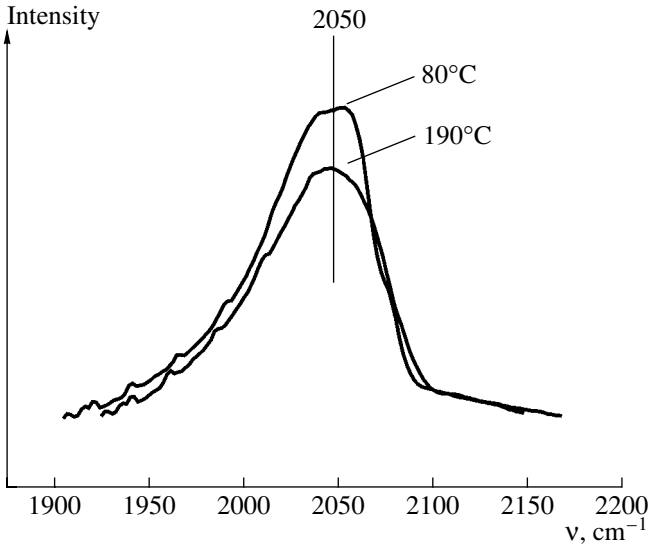

Fig. 6. Fourier transform IR spectra measured in situ in the course of CO oxidation in the presence of H_2 on the 2 vol % Pt/Al_2O_3 catalyst. The composition of the mixture at the reactor inlet, vol %: CO, 0.50; O_2, 0.55; H_2, 75; He, 23.95. Space velocity: 12000 h^{-1}.

Interpretation of Experimental Data Obtained on the 2 wt % Pt/γ-Al_2O_3 Catalyst Using In Situ IR Spectroscopy

The Pt/C catalyst was found nontransparent to IR radiation; therefore, the 2 wt % Pt/γ-Al_2O_3 catalyst was prepared and characterized in order to perform kinetic experiments. Data obtained in an XPS study of the Pt/C and Pt/γ-Al_2O_3 catalysts demonstrated that platinum occurred in a metal state in both of the catalysts. Insignificant differences in the sizes of supported platinum particles and corresponding specific surface areas were taken into account in the calculations performed by the mathematical model proposed. Moreover, these catalysts exhibited similar activities in the reaction of CO oxidation in the presence of H_2.

Figure 5 compares the experimental and theoretical temperature dependence of the values of θ_{CO}, the outlet concentration of CO, the conversion of O_2, and the selectivity for the reaction of CO oxidation in the presence of H_2 on the 2 wt % Pt/γ-Al_2O_3 catalyst. Qualitatively, the experimental data obtained on the 2 wt % Pt/γ-Al_2O_3 sample differ only slightly from the results for the 1 wt % Pt/C catalyst (see Fig. 2). The values of θ_{CO} for the surface of the 2 wt % Pt/γ-Al_2O_3 catalyst in the course of the reaction were determined from IR spectra in accordance with the above procedure. As an example, Fig. 6 shows these spectra measured in the

course of the reaction at various temperatures. It can be seen that the spectra exhibited one peak with a maximum at 2050 cm^{-1}. According to Gordon and Ford [24], this peak corresponds to the vibrations of CO molecules adsorbed on Pt metal. Note that θ_{CO}, which was determined from the IR spectra, belonged to the entire catalyst bed; thus, it is an averaged value.

As the reaction temperature was increased from 60 to 190°C, θ_{CO} changed from ~1 to 0.7. Data obtained for the 2 wt % Pt/γ-Al_2O_3 catalyst were interpreted in terms of the kinetic model considered in this section with the set of the rate constants of steps given in Table 3, as well as in the case of the 1 wt % Pt/C catalyst. Note that the averaged surface coverage with CO molecules was calculated from the equation

$$\theta_{CO} = \int_{\xi=0}^{\xi=1} \theta_{CO}(\xi)d\xi,$$

where $\theta_{CO}(\xi)$ is the calculated dependence of θ_{CO} on the catalyst bed length $\xi = L/L_0$.

As can be seen in Fig. 5, the theoretical relationships satisfactorily reproduce experimental data on a quantitative level.

In general, the calculated results allowed us to believe that the mechanism proposed for the oxidation of CO in the presence of H_2 adequately reflects the experimental kinetic data obtained on Pt-containing catalysts. In particular, the model adequately reproduces a narrow temperature region in which the deep purification of hydrogen from carbon monoxide is achieved. The data obtained allowed us to consider that the oxidation of CO and the oxidation of H_2 occur simultaneously and independently. Both of the reactions are limited by the dissociative adsorption of oxygen, whereas the selectivity primarily depends on the surface coverage with carbon monoxide and hydrogen molecules.

CONCLUSIONS

As a result of this study, we found that the Pt/C catalyst is highly active and selective in the reaction of CO oxidation in the presence of hydrogen. This catalyst can decrease the concentration of carbon monoxide in a hydrogen-containing gas from 0.6–1.0 to 10^{-4} vol % (10 ppm) over a wide range of conditions.

Based on the well-known published data on the separate oxidation of CO and H_2 on platinum, we proposed a reaction mechanism for the oxidation of carbon monoxide in the presence of hydrogen. We found that the experimental data on the oxidation of carbon monoxide in the presence of hydrogen on platinum catalysts can be quantitatively described in terms of this mechanism.

ACKNOWLEDGMENTS

We are grateful to P.G. Tsyrul'nikov, N.B. Shitova, and D.A. Shlyapin for providing us with a catalyst for studies. We are grateful to V.I. Zaikovskii for the micrographs of catalyst samples and his assistance in interpreting them. We are grateful to E.A. Paukshtis for his assistance in IR spectroscopic measurements and to A.I. Boronin and S.V. Koshcheev for performing the XPS studies of catalysts. We thank P.A. Simonov for measuring the size of Pt particles in the catalysts.

This work was supported in part by the Russian Foundation for Basic Research (project no. 03-03-33036).

REFERENCES

1. Amphlett, J.C., Mann, R.F., and Peppley, B.A., *Int. J. Hydrogen Energy*, 1996, vol. 21, no. 8, p. 673.
2. Pettersson, L.J. and Westerholm, R., *Int. J. Hydrogen Energy*, 2001, vol. 26, p. 243.
3. Brown, M.L., Green, A.W., Cohn, G., and Andersen, H.C., *Ind. Eng. Chem.*, 1960, vol. 52, no. 10, p. 841.
4. US Patent 3216783, 1965.
5. Oh, S.H. and Sinkevitch, R.M., *J. Catal.*, 1993, vol. 142, p. 254.
6. Manasilp, A. and Gulari, E., *Appl. Catal., B*, 2002, vol. 37, p. 17.
7. Schubert, M.M., Gasteiger, H.A., and Behm, R.J., *J. Catal.*, 1997, vol. 172, p. 256.
8. Son, I.H., Shamsuzzoha, M., and Lane, A.M., *J. Catal.*, 2002, vol. 210, p. 460.
9. Igarashi, H., Uchida, H., Suzuki, M., Sasaki, Y., and Watanabe, M., *Appl. Catal., A*, 1997, vol. 159, p. 159.
10. Watanabe, M., Uchida, H., Igarashi, H., and Suzuki, M., *Chem. Lett.*, 1995, vol. 24, no. 1, p. 21.
11. WO Patent 9964153, 1999.
12. Snytnikov, P.V., Sobyanin, V.A., Belyaev, V.D., Tsyrulnikov, P.G., Shitova, N.B., and Shlyapin, D.A., *Appl. Catal., A*, 2003, vol. 239, nos. 1–2, p. 149.
13. Snytnikov, P.V., Sobyanin, V.A., Belyaev, V.D., and Shlyapin, D.A., *Chem. Sustainable Dev.*, 2003, vol. 11, p. 297.
14. RF Patent 2191070, 2002.
15. RF Patent 2211081, 2003.
16. Kahlich, M.J., Gasteiger, H.A., and Behm, R.J., *J. Catal.*, 1997, vol. 171, p. 93.
17. Kim, D.H. and Lim, M.S., *Appl. Catal., A,* 2002, vol. 224, p. 27.
18. Schubert, M.M., Kahlich, M.J., Gasteiger, H.A., and Behm, R.J., *J. Power Sources*, 1999, vol. 84, p. 175.
19. US Patent 4978649, 1990.

20. Shitova, N.B., Al't, L.Ya., and Perelevskaya, I.G., *Zh. Neorg. Khim.*, 1998, vol. 43, no. 5, p. 800 [*Russ. J. Inorg. Chem.* (Engl. Transl.), vol. 43, no. 5, p. 723].
21. Van Dam, H.E. and van Bekkum, H., *J. Catal.*, 1991, vol. 131, p. 335.
22. Moulder, J.F., Stickle, W.F., Sobol, P.E., and Bomben, K.D., *Handbook of X-ray Photoelectron Spectroscopy*, Eden Prairie, MN: Perkin-Elmer, 1992.
23. *NIST X-ray Photoelectron Spectroscopy Database,* 1997.
24. Gordon, A.J. and Ford, R.A., *Chemist's Companion: A Handbook of Practical Data, Techniques, and References*, New York: Wiley, 1972.
25. Boreskov, G.K., *Geterogennyi kataliz* (Heterogeneous Catalysis), Moscow: Nauka, 1988.
26. Zhdanov, V.P. and Kasemo, B., *Appl. Surf. Sci.*, 1994, vol. 74, p. 147.
27. Hellsing, B., Kasemo, B., and Zhdanov, V.P., *J. Catal.*, 1991, vol. 132, p. 210.
28. Fassini, M., Zhdanov, V.P., Rinnemo, M., Keck, K.-E., and Kasemo, B., *J. Catal.*, 1993, vol. 141, p. 438.
29. Hellsing, B., Kasemo, B., Ljungström, S., Rosen, A., and Wahnström, T., *Surf. Sci.*, 1987, vol. 189–190, p. 851.
30. Ljungström, S., Kasemo, B., Rosen, A., Wahnstrom, T., and Fridell, E., *Surf. Sci.*, 1989, vol. 216, p. 63.